SCISPACE
formerly Typeset

Open access • Journal Article • DOI:10.1007/BF01017860

The Theory of Ostwald Ripening — Source link

Peter W. Voorhees

Institutions: National Institute of Standards and Technology

Published on: 01 Jan 1985 - Journal of Statistical Physics (Kluwer Academic Publishers-Plenum Publishers)

Topics: Ostwald ripening

Related papers:

- The kinetics of precipitation from supersaturated solid solutions
- Theory of precipitate change by redissolution
- Theory of Ostwald ripening: Competitive growth and its dependence on volume fraction
- Ostwald Ripening of Two-Phase Mixtures
- The dependence of ostwald ripening kinetics on particle volume fraction

Share this paper:

View more about this paper here: https://typeset.io/papers/the-theory-of-ostwald-ripening-313btauniw

Journal of Statistical Physics, Vol. 38, Nos. 1/2, 1985

The Theory of Ostwald Ripening

P. W. Voorhees[1]

Received August 7, 1984

Developments in the theory of Ostwald ripening since the classic work of I. M. Lifshitz and V. V. Slyozov (LS) are reviewed and directions for future work are suggested. Recent theoretical work on the role of a finite volume fraction of coarsening phase on the ripening behavior of two-phase systems is reformulated in terms of a consistent set of notation through which each of the theories can be compared and contrasted. Although more theoretical work is necessary, these theories are in general agreement on the effects of a finite volume fraction of coarsening phase on the coarsening behavior of two-phase systems. New work on transient Ostwald ripening is presented which illustrates the broad range of behavior which is possible in this regime. The conditions responsible for the presence of the asymptotic state first discovered by LS, as well as the manner in which this state is approached, are also discussed. The role of elastic fields during Ostwald ripening in solid–solid mixtures is reviewed, and it is shown that these fields can play a dominant role in determining the coarsening behavior of a solid–solid system.

KEY WORDS: Ostwald ripening; phase transformations; competitive growth; diffusion.

1. INTRODUCTION

In general, any first-order phase transformation process results in a two-phase mixture composed of a dispersed second phase in a matrix. However, as a result of the large surface area present, the mixture is not initially in thermodynamic equilibrium. The total energy of the two-phase system can be decreased via an increase in the size scale of the second phase and thus a decrease in total interfacial area. Such a process is termed *Ostwald ripening* or *coarsening*. Since the excess energy associated with the total surface area is usually small, such surface energy driven morphological changes typically manifest themselves as the last stage of a first-order phase transformation

[1] Metallurgy Division, National Bureau of Standards, Gaithersburg, Maryland 20899.

0022-4715/85/0100-0231$04.50/0 © 1985 Plenum Publishing Corporation

coalescence, which introduce new particles of a given size class, are negligible.

The flux of particles in size space is controlled by the function $\dot{R}(R)$. This function embodies much of the physics of the ripening problem, and thus must be carefully constructed. In the LS theory, $\dot{R}(R)$ was determined by examining the growth or dissolution of an isolated spherical domain into a supersaturated medium. At large supersaturations, such a Stefan problem is difficult to solve, and it is now well known that growing and dissolving spheres obey different kinetic laws.[9] However, during Ostwald ripening the supersaturation of the matrix, $\theta_m(t) \ll 1$. Therefore, the quasistationary approximation may be employed, i.e., the diffusion field in the matrix is governed by

$$\nabla^2\theta = 0 \tag{6}$$

along with the boundary conditions,

$$\theta(R) = 1/R \tag{7}$$

$$\lim_{r\to\infty} \theta(r) = \theta_m \tag{8}$$

Eq. (7) is the dimensionless form of the linearized Gibbs–Thomson equation, assuming the ideal solution, for the solute concentration in the matrix at the surface of a spherical liquid particle. As will be discussed below, if the particle or matrix is solid, Eq. (7) cannot be used. By requiring flux conservation at the matrix–particle interface and that the particle is pure solute, Eq. (6) with Eqs. (7) and (8) yields

$$\dot{R} = (\theta_m - 1/R)/R \tag{9}$$

A result of the quasistationary approximation is that this kinetic equation is valid for both growing and dissolving particles. Readily evident from Eq. (9) is its mean field nature. This is a result of employing Eq. (8) as a boundary condition, i.e., a particle grows or shrinks only in relation to a mean field concentration set at infinity.

The final element of the LS theory is mass conservation. Mass or solute conservation must be explicitly added to the theory because Eq. (9) is based on a solution to Laplace's equation, which does not conserve solute. Assuming that there are no sources of solute external to the system, solute conservation demands that the total solute content of the alloy be divided between the particle and matrix, viz.

$$\theta_0 = \theta_m(t) + \alpha f_3(t) \tag{10}$$

where θ_0 is the bulk alloy composition and $\alpha \equiv 4\pi/(3V_m c_\infty)$. The previously unknown parameter θ_m can be determined from Eq. (10), and thus θ_m couples mass conservation into the kinetic equation.

Equations (5), (9), and (10) may be rewritten as a nonlinear integrodifferential equation for the time kinetics and morphology of the ripening process. Rather than solve these equations for all times, LS found an asymptotic solution valid as $t \to \infty$. The procedure which they employed, and variants of which have appeared since, constitutes rather technical asymptotic analysis. Since a more detailed description of this procedure has been given elsewhere,[10] only the highlights will be given below.

The central idea is to reformulate the problem in terms of a double-scaled variable $\rho \equiv R/\bar{R}$ where, depending on the approach, $\bar{R}$ is either the critical radius $R_c = 1/\theta_m$, (the particle with $\dot{R} = 0$) or the maximum particle size in the system.[11] Using the reformulated kinetic equation in conjunction with the solute conservation constraint, LS showed that as $t \to \infty$, the following must be true: $K(t) = 3R_c^2\dot{R}_c \to \text{const}$, $R_c \to \bar{R}$, and $f_3 \to \theta_0/\alpha$, where $\bar{R} = f_1/f_0$. Since the rate constant K is a constant at long times, a solution of the continuity equation of the form $g(\rho)\,h(t)$ is possible, which results in an ordinary differential equation for the particle size distribution function. Moreover, the constraint that $f_3 = \theta_0/\alpha$ yields the unique value of $K = 4/9$. An interesting variant of this approach has recently been given[12,13] which employs the scaling ansatz that as $t \to \infty$, $\rho = Rt^{-x}$, and $f = f_0 t^{-y}$, where x and y are fixed by the solute conservation constraint along with the continuity and kinetic equations.

Through the above asymptotic analysis Lifshitz–Slyozov were able to make the following predictions concerning the behavior of two-phase mixtures undergoing Ostwald ripening in the long-time limit:

(1) The following temporal power laws are obeyed:

$$\bar{R}(t) = (\bar{R}^3(0) + 4t/9)^{1/3}$$

$$\theta_m(t) = (\bar{R}^3(0) + 4t/9)^{-1/3}$$

$$N(t) = \psi(\bar{R}^3(0) + 4t/9)^{-1}$$

where $\psi = \theta_0/(\alpha \int_0^{3/2} \rho^3 g(\rho)\,d\rho)$ and $t = 0$ is defined as the beginning of coarsening in the long-time regime.

(2) The asymptotic state of the system is independent of the initial conditions. Furthermore, the particle radius distribution is self-similar under the scaling of the average particle size.

(3) This time-independent distribution function $g(\rho)$ is calculable and is shown in Fig. 1.

process. However, there are clearly exceptions to such a generalization, such as the coarsening of secondary dendrite arms during the growth of a dendrite into an undercooled liquid and void growth in irradiated materials. The driving force for the ripening process is the well-known curvature dependence of the chemical potential which, assuming isotropic surface energy, is[1]

$$\mu = \mu_0 + V_m \gamma \kappa \tag{1}$$

where κ is the mean interfacial curvature and μ_0 is the chemical potential of an atom at a flat interface, V_m is the molar volume and γ is the surface energy. From Eq. (1) it is clear that atoms will flow from regions of high to low curvature. This results in the disappearance of surfaces possessing high curvature and an increase in the size scale of dispersed second phase, which is consistent with the necessary decrease in total energy of the two-phase system.

Surprisingly, the above qualitative explanation of the Ostwald ripening process seems to be all that existed for some 50 years following Ostwald's original discovery of the phenomena.[2,3] Early attempts by Greenwood[4] and Asimov[5] to construct a quantitative theory of the ripening process did not meet with success since both theories are based upon an unrealistic solution for the diffusion field in the matrix.

A major advance in the theory of Ostwald ripening was made in a paper by Lifshitz and Slyozov[6] and followed by a related paper by Wagner (LSW).[7] In contrast to previous theories, Lifshitz and Slyozov (LS) developed a method for treating an ensemble of coarsening particles, and were able to make quantitative predictions on the long-time behavior of coarsening systems without recourse to a numerical solution of the relevant equations. The LS paper stimulated much interest soon after it was published and it has become the seminal paper to which all subsequent theoretical work on Ostwald ripening has been compared. There has also been a recent resurgence in interest in the coarsening problem. I hope to illustrate the fundamental importance of the LS paper by critically examining some of these recent developments and enumerating some of the still unanswered questions.

In order to place the modern work in perspective, a brief review of the Lifshitz–Slyozov and related papers will be given. Following this, a review of recent work will be given which deals with: the effects of a finite volume fraction of coarsening phase on the ripening process, transient Ostwald ripening and the influence of elastic fields on the coarsening behavior of two-phase mixtures. Finally, directions for future research will be outlined.

Dimensionless variables will be employed for the remainder of this paper. An appropriate characteristic length for a system which exchanges

mass during coarsening, through which all quantities of length will be scaled, is the capillary length l_c defined as

$$l_c = 2\gamma V_m/(R_g T) \tag{2}$$

where R_g is the gas constant and T is temperature. A dimensionless time may also be defined as

$$t = [Dc_\infty V_m/l_c^2]\, t^* \tag{3}$$

where t^* is dimensional time, D is the diffusion coefficient, and c_∞ is the solute concentration in the matrix at a flat interface. Finally a dimensionless concentration θ will be defined as

$$\theta = (c - c_\infty)/c_\infty \tag{4}$$

Other dimensionless lengths, times, and field variables can be defined for systems which exchange heat during coarsening [8].

2. CLASSIC THEORY OF COARSENING

In this review of the LS approach, particular attention will be paid to the assumptions upon which the theory is based. A number of preliminary assumptions must be made before continuing: (1) the coarsening second phase is spherical with radius R, (2) the particles are fixed in space, and (3) both the particles and the matrix are fluids. We shall now proceed to derive the three equations upon which the LS approach is based.

The morphology of a dispersed spherical second phase will be characterized in terms of particle radius distribution, $f(R, t)$, where f is defined as the number of particles per unit volume at time t in a size class R to $R + dR$. Representing a particle radius distribution in terms of a continuous function $f(R, t)$ implies that there exists sufficient numbers of particles in the system for such a continuum approach to be valid. This assumption is not overly restrictive, since the particle densities in most coarsening systems are on the order of 10^8 to 10^{14} particles/cm^3. From the definition of f it is clear that $N(t) = f_0$, where $N(t)$ is the number of particles per unit volume, and $f_n = \int_0^\infty R^n f(R, t)\, dR$. Thus, the flux of particles passing through a size class R to $R + dR$ is $f \cdot \dot{R}$, where $\dot{R} \equiv dR/dt$. Therefore, the time rate of change of f is given by a continuity equation of the form

$$\partial f/\partial t + \partial(f \cdot \dot{R})/\partial R = J \tag{5}$$

where J is a production term in particle size space. In the LS treatment, J is set to zero, implying that processes such as nucleation and particle

different results. While the methodology used to arrive at the microscopic equations vary, the following illuminates the basic assumptions of the microscopic formulation. The coarsening phase is again assumed to be spherical and fixed in space. The emission or absorption of solute from growing or dissolving particles is modeled by placing point sources or sinks of solute at the center of each particle. Therefore, the diffusion field within the matrix obeys,

$$\nabla^2\theta = +4\pi \sum_{i=1}^{N} B_i \delta(\mathbf{r} - \mathbf{r}_i) \tag{11}$$

where the source/sink strengths B_i are unknowns and $\delta(\mathbf{r} - \mathbf{r}_i)$ is the Dirac δ function. The solution of Eq. (11) is

$$\theta = \theta_m - \sum_{i=1}^{N} B_i/|\mathbf{r} - \mathbf{r}_i| \tag{12}$$

where $\mathbf{r}$ locates a field point and $\mathbf{r}_i$ locates a particle center. The unknown constants B_i and θ_m are determined, as in the LS treatment, by requiring interfacial equilibrium and solute conservation. Specifically, in order to avoid applying the Gibbs–Thomson equation pointwise along the particle–matrix interface, it is assumed that the particles will remain spherical and Eq. (7) is applied to the surface averaged concentration of a particle. This interfacial boundary condition along with the solute conservation constraint yields the following set of boundary conditions:

$$B_j = \theta_m R_j - 1 + R_j \sum_{\substack{i=1 \\ i \neq j}}^{N} B_i/R_{ij} \tag{13}$$

$$\theta_m = \theta_0 - \alpha \sum_{i=1}^{N} R_i^3 \tag{14}$$

where $R_{ij} \equiv |\mathbf{r}_j - \mathbf{r}_i|$. Using Gauss' law and Eq. (11) one can show that $B_i = R_i^2 \dot{R}_i$. Using this result, and the previous observation that as $t \to \infty$, $\theta_m \to 0$ yields a reformulated version of Eq. (14),

$$\sum_{i=1}^{N} B_i = 0 \tag{15}$$

Eqs. (13) and (15) constitute a set of $N+1$ equations for the $N+1$ unknowns of Eq. (12). The boundary condition, Eq. (15), while being a natural outgrowth of the mass conservation constraint, is essential for guaranteeing the convergence of the summation appearing in Eqs. (12) and

(13) as $N \to \infty$. Similar equations have been studied in the theory of diffusional limited reactions,[26] and void growth in irradiated materials.[27] Wiens and Cahn[28] appear to be the first to use such equations to describe coarsening.

The objective of each of the averaging procedures employed by BW, VG, TK, and MR is to determine the statistically averaged growth rate $\dot{R}$ or a statistically averaged source/sink strength $B(R) = R^2\dot{R}$ of a given particle at a specified ϕ using Eqs. (13) and (14). Once this is known the continuity equation along with the solute conservation constraint are employed to determine the kinetics and morphology of the coarsening mixture. An overview of each of these statistical averaging procedures is given below.

Tokuyama and Kawasaki[25] statistically average Eq. (13) through a scaling expansion technique originally developed by Mori and coworkers.[29-31] The scaling approach performs spatial and temporal coarse graining over length and temporal scales characteristic to the ripening problem. An advantage of their approach is that in the thermodynamic limit, i.e., $N \to \infty$ and $V \to \infty$, $N/V \to$ const, it is possible to explicitly evaluate the magnitude of the fluctuations of $f(R, t)$. TK define three characteristic length and time scales for a first-order phase transformation process: one characteristic of a nucleation stage, a second pertaining to an intermediate growth stage where $\phi = \phi(t)$, and a third characteristic of a late or ripening stage where ϕ is constant. A discussion of the intermediate stage will be given later. They find for $(3\phi)^{1/2} \ll 1$, in the late stage regime,

$$B(\rho) = \rho - 1 - \rho(M_2 - \rho)(3\phi)^{1/2} - C(3\phi)^{1/2} \tag{16}$$

where $\rho \equiv R/\bar{R}$, $M_n \equiv \int_0^\infty \rho^n f(R, t) dR / \int_0^\infty f(R, t)\, dR$ and C is a complex function of ρ and M_n.[32] Their expression for $B(\rho)$ becomes time independent as $t \to \infty$ since $f(R, t) \to g(\rho)\, h(t)$. As a result, scale-invariant distributions exist in the long-time limit. The first two terms in Eq. (16) are simply the LSW kinetic equation in the limit $t \to \infty$ and thus as $\phi \to 0$ their theory also reproduces the LSW results. The third term is a drift term in particle size space which is independent of the diffusional interactions between particles. The fourth term is a soft collision term resulting from the diffusion interactions between particles on distances of order $(3\phi)^{1/2}/\bar{R}$. They also show that the fluctuations in $f(R, t)$ which result from diffusional interactions are consistent with the solute conservation constraint and that they are small, but observable, if the dimensionality of the system is greater than zero. In the initial TK paper, they use Eq. 16 along with the continuity equation and conclude that the scaled time-independent distributions are a function of ϕ and that the rate constant K is independent of ϕ. However, in a later paper Tokuyama, Enomoto, and Kawasaki[32] reexamine these

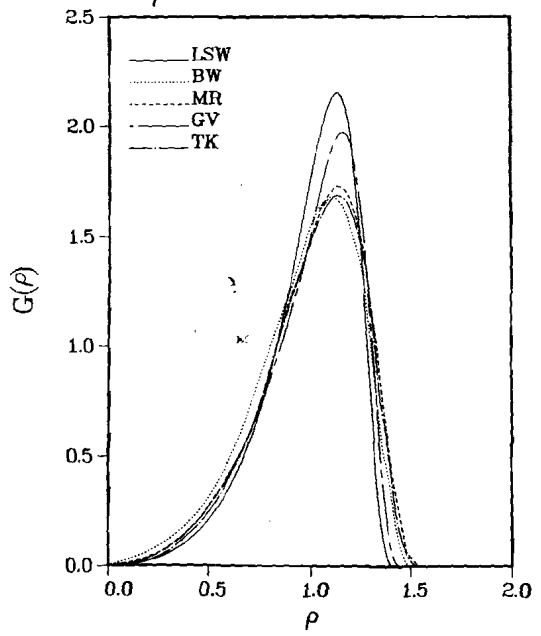

Fig. 1. Time-independent scaled particle radius distributions versus $\rho = R/\bar{R}$, where $\int_0^\infty g(\rho)\, d\rho = 1$. The distributions due to BW, MR, GV, and TK are all for $\phi = 0.1$, and the LSW distribution is for $\phi = 0$.

Perhaps the most intriguing prediction was the universal, self-similar nature of the coarsening process at long times. This universal behavior is a direct result of the influence of the solute conservation constraint on long-time solution of the continuity and kinetic equations. It is this universal self-similar nature which held out the promise of describing the Ostwald ripening process in a wide variety of two-phase mixtures. Furthermore, while some of the above temporal laws were deduced by earlier workers,[4] the LS theory gave the constants of proportionality necessary for careful comparisons between theory and experiment.

Soon after the publication of the LSW papers, many experimentalists rushed to test the veracity of the theory. Experiments have confirmed the prediction of self-similar coarsening behavior at long times; however, virtually none of the reported distributions are of the form predicted by LSW. The reported distributions are generally broader and more symmetric than the LSW predictions.[14,15] While the temporal power law for $\bar{R}$ has been confirmed in a truely convincing fashion in only a limited number of

cases,[14] no experiment has been capable of measuring the preexponential factor in any of the above equations owing to a lack of knowledge of the relevant materials parameters. Furthermore, there also appears to be a volume fraction dependence of the rate constant K, although the experimental results are not completely convincing.[14,16]

3. MODERN COARSENING THEORY

It was realized early that a major problem with the LSW approach was the mean field nature of the kinetic equation, Eq. (9). Such a mean field approximation assumes that a particle's coarsening rate is independent of its surroundings, i.e., a particle with nearest neighbors which are larger than itself will coarsen at exactly the same rate as if it were surrounded by particles that were of a smaller radius. LS assumed that their deterministic rate equation would be valid at an unspecified low volume fraction of coarsening phase, ϕ. This flaw in the LS approach was almost immediately recognized, and advanced as the cause for the apparent disagreement between the theoretically predicted and experimentally measured particle size distributions.[17] More recently, a direct experimental measurement of individual particle coarsening rates was undertaken.[18] This work clearly showed that at volume fractions as low as 3% individual particle coarsening rates were in fact not a smooth function of particle radius as predicted by Eq. (9), but varied according to a particle's local environment. The surprising strength of these diffusional interactions between particles stems from the long range Coulombic nature of the diffusion field surrounding a particle. As a result, particle interactions occur at distances of many particle diameters and restrict the validity of the LS theory to the unrealistic limit of zero volume fraction of coarsening phase.

In order to remove the zero volume fraction assumption of the LSW theory, one needs to determine the statistically averaged diffusional interaction of a particle of a given size class with its surroundings. Many of the attempts to determine the statistically averaged growth rate of a particle either do not not account for the long-range nature of the diffusion field surrounding the particle,[4,17,19] and/or employed and hoc assumptions in an attempt to account for the diffusional interactions between particles.[5,20] Recently, Brailsford and Wynblatt (BW),[21] Voorhees and Glicksman (VG),[8,22] Glicksman and Voorhees (GV),[23] Marqusee and Ross (MR),[24] and Tokuyama and Kawasaki (TK),[25] have proposed more realistic models of the coarsening process at finite-volume fractions of coarsening phase.

Interestingly, each of these groups used identical microscopic equations with which the statistical averaging is performed, yet arrive at quantitatively

$a > R$, and allowing solute production in the surrounding medium. However, BW do not employ a fully self-consistent approach and instead use a simple interpolation formula for mathematical simplicity, which yields the following rate equation in the long-time limit,

$$B(\rho) = (\xi\rho - 1)(1 + \xi q\rho) \tag{18}$$

where $\rho = R/\bar{R}$, $\xi = \bar{R}/R_c$ and q is a function of ϕ and various moments of $g(\rho)$. Again, $B(\rho)$ is time independent, since $\bar{R}$ and R_c have the same time kinetics as $t \to \infty$. Also, the BW theory reduces to the LSW limit since as $\phi \to 0$, $q \to 0$. Performing a similar asymptotic analysis as Lifshitz and Slyozov, Eq. (18) yields the results shown in Figs. 1 and 2.

Voorhees and Glicksman[8,22] employ Eqs. (13) and (15) along with computer simulation techniques to perform the statistical averaging. Large numbers of particles, $\sim 10^2$, are placed at random locations in a basis, and then the basis is translated via cubic lattice translation vectors to fill all space. The periodic nature of the particle arrangement allows Eq. (13) to be reformulated into two rapidly and absolutely convergent summations using lattice summation techniques originally developed by Ewald.[37] At finite ϕ, the coarsening particles interact diffusionally, which results in fluctuations in individual particle coarsening rates as shown in Fig. 4. Note that the fluctuations are smaller for the small particles in the dispersion indicating that, as expected from Eq. (13) in the limit $R_i \to 0$, small particles interact weakly with their immediate neighbors. Averaging these fluctuations over a given size class yields the discrete B_i values shown in Fig. 3. Using the physical insight obtained from the simulations, GV[23] constructed a simple effective medium which reproduces the $B(\rho)$ and rate constant data derived from the simulations over $0.05 \leqslant \phi \leqslant 0.5$. The GV effective medium approach involves placing a representative particle inside an averaging sphere of radius a, where $a = 1/\phi^{1/3}$ for $\rho \leqslant \rho_c$ and $a = R/\phi^{1/3}$ for $\rho \geqslant \rho_c$, where $\rho = R/\bar{R}$ and $\rho_c = R_c/\bar{R}$. Assuming interfacial equilibrium, and that the concentration at the surface of the averaging sphere is a functional of $g(\rho)$, yields the following kinetic equation:

$$\begin{aligned} B(\rho) = {} & (\alpha'\rho - 1)(1 + \alpha'\phi^{1/3}\rho)\, S(\rho_c - \rho) \\ & + (\alpha'\rho - 1)(1 + \phi^{1/3})\, S(\rho - \rho_c) \end{aligned} \tag{19}$$

where α' is a functional of the moments of $g(\rho)$ and $S(x)$ is a step function defined as 0 for $x < 0$ and 1 for $x > 0$. Clearly as $\phi \to 0$ the LSW result is recaptured and $B(\rho)$ is time independent, since α' is only a function of ϕ. The GV kinetic equation at $\phi = 0.1$ is shown in Fig. 3. Asymptotic analysis of the scaled continuity equation and mass conservation constraint yields the results shown in Figs. 1 and 2.

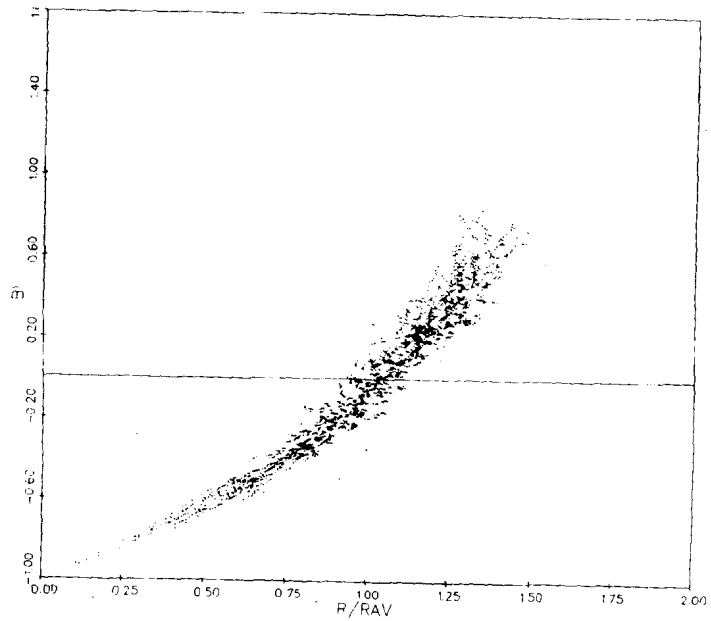

Fig. 4. Discrete $B(\rho)$ data at $\phi = 0.1$ derived from the simulations of VG. The scatter in the value of B_i for a given particle size is a result of diffusional interactions or "soft collisions" between particles which occur at finite ϕ.

All of the theories are in general agreement on the following points: (1) the temporal power laws originally reported by LS are not a function of ϕ; however, the amplitude of the power laws is ϕ dependent; (2) scaled time invariant distribution functions exist at finite ϕ in the long-time limit; (3) as ϕ increases, the time invariant distributions become broader and more symmetric than the LSW distribution; (4) the rate constant rises rapidly at low ϕ and is followed by a slower increase with ϕ; (5) the predictions for $K(\phi)$ of GV and MR are almost identical up to $\phi \sim 0.1$, as shown in Fig. 2; and (6) the $B(\rho)$ functions of MR and GV are quite similar and in agreement with the VG simulation data, all three descriptions showing increased diffusional interactions with increasing ϕ which result in an increase in the absolute value of the statistically averaged coarsening rate of a particle in a given size class. Note that the mathematical similarity between the $B(\rho)$ functions predicted by BW and MR is deceiving, since the values of the numerically determined parameters in each theory will be different.

equations and find that both K and $g(\rho)$ are functions of ϕ. The time-independent scaled distribution function found by setting $C=0$ is shown in Fig. 1.

Marqusee and Ross[24] determine the statistically averaged kinetic equation via a multiple scattering approach.[33-35] The basic idea is to write the microscopic equations, Eqs. (13) and (12), in the form of a multiple scattering series and average the resulting equations, assuming particle positions are independent. By summing the most divergent terms in the scattering series they arrive at an expression for the statistically averaged kinetic equation. They conclude that in the long-time limit,

$$B(\rho) = (a_0\sigma_1\rho - 1)(1 + a_0\rho(3\phi N_0 a_0)^{1/2}) \tag{17}$$

where $\rho = R/\bar{R}$, σ_1 and N_0, are the amplitudes of the temporal power laws for $\theta_m(t)$ and $N(t)$, respectively, in the long-time limit and $a_0 = K^{1/3}$. The rate constants N_0 and σ_1 are determined by employing the time-independent continuity equation valid in the long-time limit and mass conservation. As with TK, and $\phi \to 0$, $a_0 = 1/\sigma_1$ and the LSW distribution and time kinetics are recaptured. Also, $B(\rho)$ is time independent at all volume fractions. Furthermore, for $\phi \leqslant 0.01$ a perturbation treatment predicts that $K(\phi) - K(0) \sim \phi^{1/2}$. Numerical evaluation of a_0, σ_1, and N_0 yields the particle size distribution shown in Fig. 1 along with $K(\phi)$ shown in Fig. 2. The MR kinetic equation, at $\phi = 0.1$, is also shown in Fig. 3.

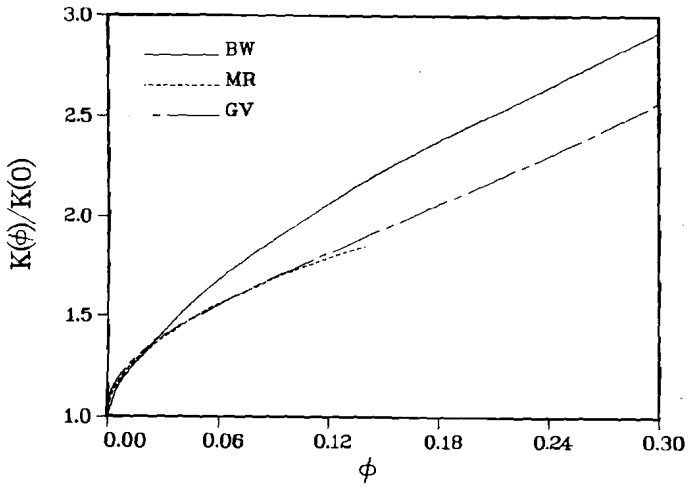

Fig. 2. The rate constant $K(\phi)$ relative to $K(0)$ versus the volume fraction ϕ.

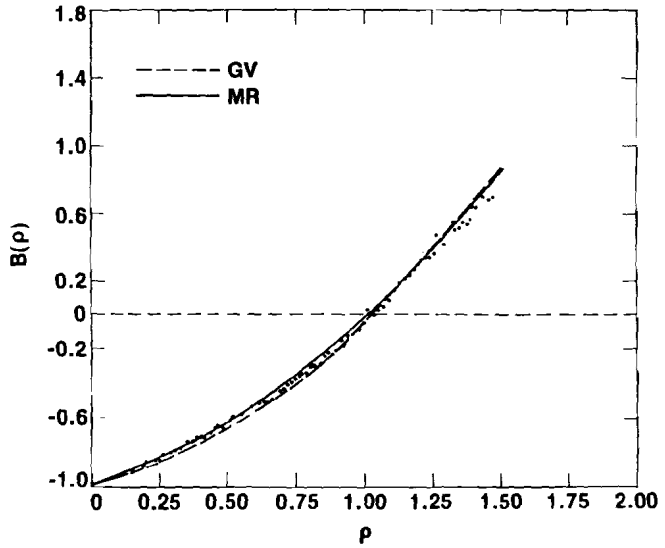

Fig. 3. The sink strength $B(\rho) = R^2\dot{R}$ versus ρ at $\phi = 0.1$. The data points shown are the discrete simulation results of VG which were computed by averaging the B_i data shown in Fig. 4. The smooth GV curve was determined using their effective medium approach. For comparison, the LS kinetic equation is $B(\rho) = \rho - 1$. The nonlinearity of the $B(\rho)$ data indicates that diffusional interactions between particles results in an increase in the absolute value of the statistically averaged coarsening rate of a particle.

Brailsford and Wynblatt[21] employ chemical rate theory to determine the statistically averaged growth rate of a particle. Despite the seemingly *ad hoc* nature of the chemical rate theory, this model cannot be discounted outright. For example, Brailsford has shown[27] that in the limit of a monodispersion, i.e., diffusion to a random array of absorbing sinks, a statistical average of equations similar to Eq. (13) agree with the predictions of the BW effective medium approach. Also the specific predictions of the variation of a particle sink strength with ϕ derived using the BW effective medium approach in the monodisperse limit are quite similar to those reported for diffusion-controlled reactions.[36] There are also marked similarities between the MR and BW approaches. The basic idea of the homogeneous rate theory is that a statistically average sense, the emission of solute from all the particles in the dispersion can be represented by a homogeneous production rate in the same medium. The emission rate and sink strength of a particle can be determined self-consistently by placing a representative particle of a given size class inside a sphere of radius a where

$t = 0$ is *not* the beginning of self-similar coarsening). If the matrix concentration θ_m is represented by $\zeta(t)/\bar{R}$, Eqs. (20), (21), and (22) yield

$$\begin{aligned} \dot{\theta}_m(0) &= -3\alpha f_0 |\zeta - 1| \\ \dot{\bar{R}}(0) &= A|\zeta/2 - 1|/(f_0\beta^2) \\ \dot{N}(0) &= \dot{f}_0 = 0 \\ \dot{I}(0) &= 4\pi A|3\zeta - 4|/\beta^3 \end{aligned} \tag{23}$$

where $I \equiv$ the total interfacial area $= 4\pi f_2$. The time-dependent parameter ζ is a measure of the degree of matrix supersaturation relative to the average particle size and, in general, $\zeta(t) \geqslant 1$; and $\zeta \to 1$ as $t \to \infty$. As a result, $\dot{\theta}_m \leqslant 0$ and since $\dot{\phi} = -\dot{\theta}_m$, $\dot{\phi} > 0$ for all assumed initial supersaturations. This implies that the matrix concentration will always initially decrease with time and ϕ will always initially increase. However, if $\zeta \geqslant 2$, $\dot{I}$, and $\dot{\bar{R}} > 0$, indicating that on average the particles are growing into a super-saturated medium. However, $\dot{I}$ must be less than zero since an Ostwald ripening process is a surface-energy-driven morphological change. As a result, $\zeta < 4/3$ in the coarsening regime. Interestingly, if $1 \leqslant \zeta \leqslant 4/3$, $\dot{\bar{R}} \leqslant 0$, and thus $\bar{R}$ is constrained to decrease initially and, furthermore $\dot{\bar{R}}$ and $\dot{R}_c$ are of opposite signs. Contrast these results with a self-similar coarsening process where $\dot{\bar{R}} > 0$ and $\bar{R} = R_c$. Clearly, the entire time evolution of such a distribution requires a more complete solution of the integrodifferential equation. Nevertheless, the above analysis illustrates the richness of the equations and the unexpected results which are possible.

By far the most complete study of ripening in the fully time-dependent regime was undertaken by Venzl.[39] Venzl solved the time-dependent nonlinear integrodifferential equation in the limit of $\phi = 0$. Using a relatively restricted set of initial conditions, Venzl showed that the LSW distribution was indeed a unique attractor state for the nonlinear dynamical system. The presence of this attractor state appears to be a direct result of the solute conservation requirement, as asserted by LS. His results also show that the path by which these particle radius distributions took to the asymptotic state is not fully constrained at all times, but depends on the initial conditions. The path dependence of a distribution's approach to the scale-invariant regime has important ramifications if the materials parameters of the system of interest dictates a slow coarsening rate, for then the morphology of the two-phase dispersion cannot be predicted for any experimentally accessible times without knowledge of the initial state. Such systems have been studied by Vedula and Heckel[40] and Watanabe and Masuda.[41] Venzl also showed that distributions which are narrower than the time-invariant form tended to, at first, become broader than this distribution. Furthermore, it is clear from his results that it is possible to have $\dot{\bar{R}}^3 \approx K$ when the scaled particle size distribution function is not time invariant. Therefore, it would be difficult to determine experimentally if self-similar coarsening has occurred by only measuring $\bar{R}(t)$.

Other less complete theoretical studies of transient coarsening tend to corroborate Venzl's conclusions. MR,[13] using a scaling ansatz originally suggested by Binder,[12] also show that the approach to the asymptotic state is not fully constrained. TK[25] show that there is an intermediate stage during a first-order phase transformation process where $\phi = \phi(t)$. In this regime the particle radius distribution is not time independent but does obey a scaling relationship, and more importantly $\bar{R}$ is proportional to $t^{1/3}$. Recent experiments have also reported $\bar{R}$ is proportional to $t^{1/3}$ when $\phi = \phi(t)$,[42] although the results are not completely convincing due to experimental error. VG performed computer simulations in the transient regime and also report in agreement with the above: (1) a nonconstrained approach of the particle radius distribution to the asymptotic state, (2) that distributions which are much broader than the scaled time-independent distribution evolve slowly toward this distribution, (3) particle size distributions which are initially narrower than the scaled time-independent distribution tend to at first become broader than the time-independent shape, and (4) it is possible for $\bar{R}$ to decrease initially when $\dot{N} = 0$.

In summary, the LSW distribution does appear to be a unique attractor state for the nonlinear integrodifferential equation describing the time evolution of a particle radius distribution. Consistent with LS, the solute conservation constraint plays a central role in the presence of this attractor state. It is also possible that many of the reports of particle size distributions which have longer tails for $R > \bar{R}$ than those predicted theoretically are a result of the extremely long time required for a very broad scaled particle radius distribution to become the time invariant.

5. THE EFFECTS OF ELASTIC FIELDS DURING OSTWALD RIPENING

It has long been recognized that elastic fields can be important in first-order phase transformations in solid–solid systems.[43,12] In fact, the classic Gibbs–Thomson equation is not valid in solid–solid systems due to: the presence of a crystalline lattice, the ability of solids to withstand nondilatational stresses, and the possibility of interfacial stresses which are different than the interfacial energy. As a result, one must question the validity of applying the LS theory, or any of the more recent finite ϕ coarsening theories, to solid–solid systems. Experimental examples of the importance of elastic fields during coarsening abound; for example,

However, disagreements exist between each of these theories:

(1) The disagreement between the $K(\phi)$ predictions of BW and those of both GV and MR most likely stems from BW's use of an *ad hoc* linear interpolation formula. It would be interesting to see what would be the predictions of a fully self-consistent chemical rate theory.

(2) The theory of GV disagrees with MR for $\phi < 10^{-3}$ since MR predict that $K(\phi) - K(0) \sim \phi^{1/2}$, and the GV effective medium approach predicts that $K(\phi) - K(0) \sim \phi^{1/3}$. However, since simulations were not performed at these low volume fractions, and the GV effective medium approach is valid *only* insofar as it reproduces the simulation results, such a disagreement is not serious. Despite this, it would be interesting if simulations could be performed at very low ϕ in order to settle the apparent disagreement.

(3) TK claim that the small difference between the rate constants predicted by TK and MR[32] results from the MR $B(\rho)$ function violating the conservation of mass constraint. However, it is not clear why this should be so, since the unknown parameters in the MR $B(\rho)$ function are specifically chosen to conserve mass.

(4) The disagreement between the $K(\phi)$ prediction of GV, and MR at $\phi \geqslant 0.12$ results from a breakdown in the assumptions employed by MR; i.e., MR assume that there are no spatial correlations between particles. The simulations performed by VG indicate that spatial correlations begin to occur at $\phi \sim 0.1$. Therefore, extension of the MR theory above $\phi \sim 0.1$ is probably unwarranted.

(5) TK insist that to order $(3\phi)^{1/2}$ soft collision terms must be present in the $B(\rho)$ function. As seen in Fig. 4, VG's simulations also suggest that these collision processes must be present and play an important role in the coarsening process. Such collision processes were ignored in the MR treatment.

(6) The similarity between the MR and GV $B(\rho)$ predictions is a little misleading, as evidenced by the dissimilarity in the predictions of the time-invariant distribution functions. This dissimilarity is a result of the different functionality of $B(\rho)$ at $\phi = 0.1$.

Although the aforementioned theories are by far the most realistic theories of Ostwald ripening yet developed, they are only in qualitative agreement on the role of finite volume fractions on the coarsening behavior of two-phase systems. Unfortunately, a crucial experiment has not been performed at low ϕ in order to compare to the theories. Work at higher ϕ is in qualitative agreement with the aforementioned theoretical predictions, i.e., time-independent distribution functions which are broader and more

symmetric than the LS form[14] and a rate constant which is relatively insensitive to changes in ϕ above approximately 0.1.[38] Surprisingly, to the best of my knowledge a coarsening experiment has never been done using a system for which all the relevant materials parameters were known *a priori*. Such an approach would permit a direct measurement of $K(\phi)$. Clearly more experimental and theoretical work is necessary in order to settle the subtle disagreements now existing between the various Ostwald ripening theories.

4. TRANSIENT OSTWALD RIPENING

There has been very little study of the behavior of coarsening systems in the transient or short-time regime. This is particularly unfortunate because LS's prediction that the asymptotic long-time solution is unique and independent of the initial conditions, i.e., that the nonlinear integrodifferential equation has a unique attractor state at long times, is one of the most intriguing aspects of the theory. It is also of fundamental importance in applying coarsening theory to experiments, for it is very possible that in many systems it is impossible to reach the long-time limit in any experimentally accessible times.

Solving the fully time-dependent coarsening problem is a formidable task. However, some insight into the nature of transient coarsening can be obtained by examining the time dependence of various moments of $f(R, t)$. Assuming, for simplicity, the LSW kinetic equation, Eq. (9), and transforming the integral of Eq. (5) (with $J = 0$) by integrating by parts yields an expression for the time rate of change of the nth moment of f as

$$\dot{f}_n = \lim_{R \to 0} (f \cdot \dot{R}) R^n + \theta_m n f_{n-2} - n f_{n-3} \tag{20}$$

assuming $f \to 0$ as $R \to \infty$. Differentiating the solute conservation constraint with respect to time, using the continuity equation, and integrating by parts yields the time rate of change of the matrix concentration as

$$\theta_m = -3\alpha[\theta_m f_1 - f_0] \tag{21}$$

To determine the time rate of change of the f_n and θ_m, it is necessary to choose an initial distribution. We shall assume a relatively simple particle size distribution of the form

$$f(R, 0) = AR^3 \exp(-\beta R) \tag{22}$$

where the constants A and β are chosen to satisfy the solute conservation constraint and specify an initial average particle size (note that in this case

elasticity and diffusion problem. Both must be solved simultaneously since both the elastic and diffusion fields are functions of particle size and separation, and are coupled through thermodynamics.[49,50]

6. CONCLUSIONS

Although the original LS paper represented a considerable advance in the theory of Ostwald ripening, it was not capable of describing coarsening in realistic two-phase mixtures. Much of the recent work reviewed herein has brought us closer to that goal, but there remain many important unanswered questions:

(1) Extensions of the theories to yet higher ϕ may prove difficult. Although this has been done using computer simulations, which enable one to avoid the spatial correlation problems algorithmically, it is not clear whether the diffusion solution upon which all these theories are based is valid at higher volume fractions. For example, preliminary work[18] on a simple two-particle model similar to that employed by Samson and Deutch[51] and Goldstein,[52] with boundary conditions appropriate to the Ostwald ripening problem, shows that as the two particles of different radius approach each other, diffusional interactions introduce nonzero components in the spherical harmonics of the particle shapes, thus violating the assumption of particle sphericity and fixed spatial locations of the particles. Furthermore, as the particles approach each other the two-p icle model predicts that the coarsening rate of both particles diverges, whereas the point source approximation, Eq. (11), does not. It is possible that these difficulties disappear following the statistical averaging performed in the simulations,[53] but this has not been proved. Nevertheless, the simulations constitute the most accurate predictions of the behavior of ripening systems at high volume fractions, and it would be most interesting if the theories of MR or TK could be extended for purposes of comparison. A related question is: What is the effect of nonspherical particles on the coarsening behavior of two-phase systems?

(2) The role of spatial correlations between particles has been largely ignored. At $\phi \neq 0$, diffusional interactions between particles are present and thus the spatial distribution of particles becomes important. All the theories reviewed assume a random spatial distribution of particles. Are such random spatial distributions found in nature? Will a highly nonrandom spatial distribution of particles eventually coarsen to a random distribution? Will a nucleation and growth process result in such a random spatial distribution? (This is certainly not the case if inhomogeneous nucleation is present.) What are the conditions under which a random spatial distribution will coarsen to a highly correlated spatial distribution? Is the appearance of time-independent scaled particle radius distributions inherently linked to the assumption of a random distribution of particles? Does a nonrandom spatial distribution of particles strongly influence a system's approach to the long time attractor state?

(3) In any two-phase mixture one phase of which is a solid, the surface energy will be anisotropic to some degree. At finite ϕ, what effect does surface energy anisotropy have on both individual particle coarsening rates, and the stochastic aspect of the ripening problem? Does the surface energy anisotropy by itself introduce a spatial directionality into the ripening problem?

(4) What particle size distribution results from a nucleation and growth process? How does this distribution influence the coarsening system's approach to the asymptotic state?

(5) What role does elasticity play in the coarsening process? Unfortunately, there is no theory which treats the linked stochastic elasticity and diffusion problem which enables prediction of both the kinetics and particle size distributions during ripening. What causes precipitate alignment in solid–solid systems? What are the conditions under which stable monodisperse ensembles of precipitates exist?

(6) Second phase domains with both positive and negative curvatures are quite common in nature, e.g., solid dendrites which grow from a supercooled melt. How do these structures coarsen under conditions of diffusional mass transfer? Do scale-invariant distributions of curvature exist in such topologically complex structures? Can the evolution of curvature which is initially both positive and negative be described by temporal power laws?

ACKNOWLEDGMENTS

It is my pleasure to acknowledge many helpful discussions with Drs. J. W. Cahn, S. R. Coriell, M. E. Glicksman, W. C. Johnson, and R. J. Schaefer. I also express my appreciation to Professor W. C. Johnson and Dr. S. R. Coriell for their comments on a preliminary version of this paper. In addition, I thank Dr. J. A. Marqusee for supplying the Marqusee and Ross distribution function, shown in Fig. 1.

REFERENCES

1. W. W. Mullins, in *Metal Surfaces*, Vol. 17, (American Society for Metals, 1962).
2. W. Ostwald, *Z. Phys. Chem.* 37:385 (1901).
3. W. Ostwald, *Analytisch Chemie*, 3rd ed. (Engelmann, Leipzig, 1901), p. 23.
4. G. W. Greenwood, *Acta. Met.* 4:243 (1956).
5. R. Asimov, *Acta. Met.* 11:72 (1962).

precipitates have been shown to line up in raftlike structures and change shape during ripening.[44] Very recent progress illuminating the role of elasticity during Ostwald ripening has been made. In fact, it now appears possible that the coupled stochastic elastic and diffusion problem can be treated self-consistently to yield a realistic theory of Ostwald ripening in solids.

Solid precipitates in a solid matrix differ from liquid precipitates in a liquid matrix in many ways all of which have a great impact on the ripening behavior of the two-phase mixture. In particular, the lattice parameters of the precipitate and the matrix are usually different and in certain cases the lattice planes of the precipitate and the matrix are continuous across the matrix–particle interface. A result of such a coherent interface is that long-range elastic fields are generated in both the precipitate and matrix phases. In addition, the differences in atomic radii of the solute and solvent atoms also introduce elastic stress fields. The importance of these elastic fields is that they couple to the composition field and thus influence the coarsening behavior of precipitates. An example of the effects of both precipitate and compositionally generated stress fields is shown in Fig. 5. The equilibrium composition fields shown are a result of both the elastic interactions between the two coherent precipitates with different elastic constants than the matrix, and the nonuniform composition field.[45] Since the system is at equilibrium this nonuniform composition field does not engender mass flow. This also demonstrates that the effective materials parameter approach of LS,[6] which cannot account for such an effect, is invalid. Clearly, one cannot blindly apply theories developed for fluid–fluid mixtures to solid two-phase mixtures.

Much of the theoretical work to date on the role of elasticity during Ostwald ripening has dealt only with the energetics of the coarsening process.[44,46,47] The most realistic of these models is one due to Johnson[48] which is based on a rigorous solution to the elastic problem of two elastically interacting coherent misfitting precipitates with different elastic constants than the matrix. Johnson showed that for certain combinations of materials parameters, particle sizes, and particle separations a small precipitate will grow at the expense of a larger precipitate and result in a stable monodispersion. This result can be qualitatively understood as follows. If the precipitates are softer than the matrix, as Eshelby[44] originally proved, the elastic interaction energy is negative. Since the total elastic interaction energy is proportional to $V_1 + V_2$, where V_1 is the volume of precipitate one and V_2 is the volume of precipitate two and the total surface energy is proportional to $V_1^{2/3} + V_2^{2/3}$, the negative elastic interaction energy can stabilize the precipitates against coarsening (with the constraint that $V_1 + V_2 = \text{const}$). Such a result is clearly contrary to standard capillarity controlled ripening theory, and reflects the important role stress

can play during the coarsening process in solid–solid systems. Unfortunately, the above approach, being based upon energetics, cannot provide any insight into the kinetics of the ripening process in systems where stress is important.

Clearly, elastic fields can radically change the entire late stage phase transformation process. A more realistic treatment of coarsening in solid–solid systems involves the solution of a challenging coupled stochastic

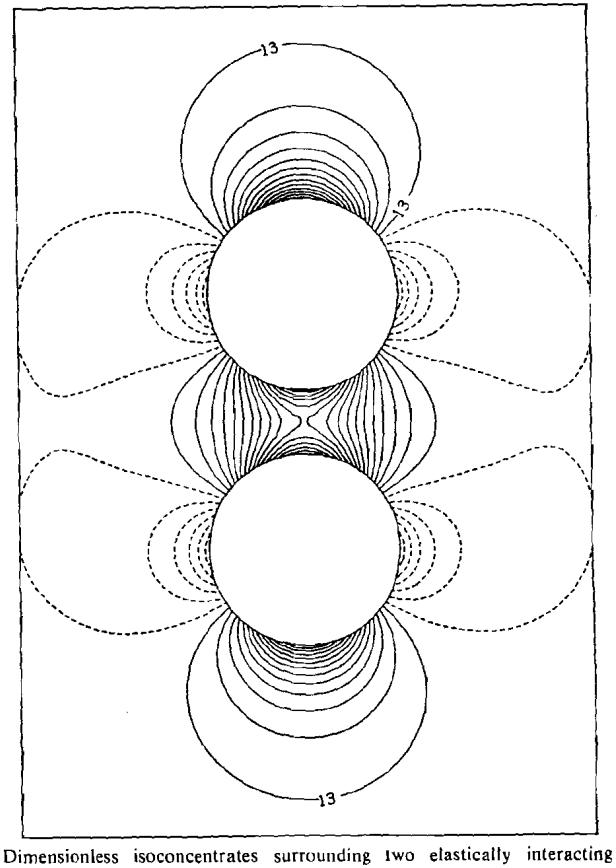

Fig. 5. Dimensionless isoconcentrates surrounding two elastically interacting coherent misfitting precipitates. In systems where the misfit is positive, the precipitates are harder than the matrix, and the atomic volume of the solute is greater than that of the solvent, solute enhancement, relative to the bulk composition, is denoted by the solid lines and solute depletion is denoted by the dashed lines. The magnitude of the change in solute concentration near the precipitates can be ~100% in certain systems. The contours are at equal normalized concentration intervals of 5.8×10^{-4}.[45]

6. I. M. Lifshitz and V. V. Slyozov, *J. Phys. Chem. Solids* **19**:35 (1961).
7. C. Wagner, *Z. Elektrochemie* **65**:581 (1961).
8. P. W. Voorhees and M. E. Glicksman, *Acta. Met.*, in press.
9. Howard B. Aaron, Dora Fainstein, and Gerald R. Kotler, *J. Appl. Phys.* **41**:4404 (1970).
10. E. M. Lifshitz and L. P. Pitaevskii, *Physical Kinetics* (Pergamon Press, London, 1981), p. 432.
11. R. D. Vengrenovitch, *Acta. Met.* **30**:1079 (1982).
12. K. Binder, *Phys. Rev. B* **15**:4925 (1977).
13. J. A. Marqusee and John Ross, *J. Chem. Phys.* **79**:373 (1983).
14. Chan Hyoung Kang and Duk N. Yoon, *Met. Trans. A* **12A**:65 (1981).
15. Y. Masuda and R. Watanabe, in *Sintering Processes*, *Materials Science Research*, Vol. 13, G. C. Kuczynski, ed. (Plenum, New York, 1979), p. 3.
16. C. K. L. Davies, P. Nash, and R. N. Stevens, *J. Mat. Sci.* **15**:1521 (1980).
17. A. J. Ardell, *Acta. Met.* **20**:61 (1972).
18. P. W. Voorhees and R. J. Schaefer, unpublished.
19. C. K. L. Davies, P. Nash, and R. N. Stevens, *Acta. Met.* **28**:179 (1980).
20. K. Tsumuraya and Y. Miyata, *Acta. Met.* **31**:437 (1983).
21. A. D. Brailsford and P. Wynblatt, *Acta. Met.* **27**:489 (1979).
22. P. W. Voorhees and M. E. Glicksman, *Acta. Met.*, in press.
23. M. E. Glicksman and P. W. Voorhees, unpublished.
24. J. A. Marqusee and John Ross, *J. Chem. Phys.* **80**:536 (1984).
25. M. Tokuyama and K. Kawasaki, *Physica* **123A**:386 (1984).
26. B. V. Felderhoff and J. M. Deutch, *J. Chem. Phys.* **64**:4551 (1976).
27. A. D. Brailsford, *J. Nuc. Mat.* **60**:257 (1976).
28. J. J. Weins and J. W. Cahn, in *Sintering and Related Phenomena*, G. C. Kuczynskie, ed. (Plenum, London, 1973), p. 151.
29. H. Mori, *Prog. Theor. Phys.* **53** (1975).
30. H. Mori and J. K. McNeil, *Prog. Theor. Phys.* **57**:770 (1977).
31. M. Tokuyama and H. Mori, *Prog. Theor. Phys.* **56**:1073 (1976), **58**:92 (1977).
32. M. Tokuyama, Y. Enomoto, and K. Kawaski, preprint.
33. M. Muthukumar and R. E. Cukier, *J. Stat. Phys.* **26**:456 (1981).
34. M. Bixon and R. Zwanzig, *J. Chem. Phys.* **75**:2359 (1981).
35. M. Tokuyama and R. I. Cukier, *J. Chem. Phys.* **76**:6202 (1982).
36. Daniel F. Calef and J. M. Deutch, *Ann. Rev. Phys. Chem.* **34**:394 (1983).
37. P. P. Ewald, *Ann. Phys. (Leipzig)* **64**:253 (1921).
38. D. J. Chellman and A. J. Ardell, *Acta. Met.* **22**:577 (1974).
39. G. Venzl, *Ber. Busenges. Phys. Chem.* **87**:318 (1983).
40. K. M. Vedula and R. W. Heckel, *Met. Trans.* **1**:9 (1970).
41. Ryuzo Watanbe, Karou Tada, and Yoshimichi Masuda, *Z. Metallkunde* **67**:619 (1970).
42. H. Wendt and P. Hansen, *Acta. Met.* **31**:1649 (1983).
43. J. W. Cahn, *Acta. Met.* **9**:795 (1961).
44. A. J. Ardell and R. B. Nicholson, *Acta. Met.* **14**:1295 (1966).
45. W. C. Johnson and P. W. Voorhees, *Met. Trans.*, in press.
46. A. G. Khachaturyan and G. A. Shatalov, *Phys. Status Solidi (A)* **26**:61 (1974).
47. V. Perovic, G. R. Purdy, and L. M. Brown, *Acta. Met.* **27**:1075 (1979).
48. W. C. Johnson, *Acta. Met.* **32**:465 (1984).
49. F. C. Larche and J. W. Cahn, *Acta. Met.* **21**:1050 (1973).
50. F. C. Larche and J. W. Cahn, *Acta. Met.* **30**:1835 (1982).
51. Rene Samson and J. M. Deutch, *J. Chem. Phys.* **67**:847 (1977).
52. Martin Goldstein, *J. Cryst. Growth* **3**:599 (1968).
53. M. E. Glicksman, private communication.

Journal of Statistical Physics, Vol. 38, Nos. 1/2, 1985

On Galvanomagnetic Size Effects in Metals

V. G. Peschanskii[1]

Received February 9, 1984

The importance of open electron trajectories formed by specular reflections of charge carriers by the sample boundary to the metal electric conductivities in the strong magnetic field H is analyzed. It is shown that the electric conductivity of the near-surface layer σ_{skin} is rather sensitive to the state of the conductor surface. The electron–hole Umklapp processes during the surface scattering of charge carriers do not change the dependence $\sigma_{skin}(H)$, while skipping from the closed Fermi surface section to the open one is able to affect σ_{skin} essentially only in bulk samples. The method is proposed to restore the indicatrix of conduction electron scattering by the sample boundary through an experimental investigation of the Sondheimer effect and the static skin effect.

KEY WORDS: Static skin effect; Umklapp surface scattering; indicatrix of conduction electron scattering; open electron trajectories; high magnetic field.

The theory of galvanomagnetic phenomena in metals developed by I. M. Lifshitz and his co-workers[1,2] for an arbitrary energy–momentum relationship for charge carriers lays the groundwork for investigations of the topology of the electron energy spectrum. The sensitivity of galvanomagnetic characteristics of metals to the Fermi surface (FS) topology is accounted for by the fundamental difference between the dynamics of free electrons and that of conduction electrons belonging to open FS sections whose drift does not coincide with the direction of the magnetic field **H**. The presence of a thin layer of such sections essentially changes the electric conductivity of a metallic sample in high magnetic fields when the trajectory curvature radius r of an electron is much smaller than its mean free path l. As the thickness of the open orbit layer related to the Fermi momentum exceeds the $(r/l)^2$ value,

[1] Institute for Low Temperature Physics and Engineering, UkrSSR Academy of Sciences, Kharkov, USSR.

822/38/1-2-17

0022-4715/85/0100-0253$04.50/0 © 1985 Plenum Publishing Corporation